

## Original Research Communication

# Structural Stabilization in Tetrameric or Polymeric Hemoglobin Determines Its Interaction with Endogenous Antioxidant Scavenger Pathways

PAUL W. BUEHLER,<sup>1</sup> FLORENCE VALLELIAN,<sup>2</sup> MALGORZATA G. MIKOLAJCZYK,<sup>1</sup>  
GABRIELE SCHOEDON,<sup>2</sup> THOMAS SCHWEIZER,<sup>3</sup>  
ABDU I. ALAYASH,<sup>1</sup> and DOMINIK J. SCHAEER<sup>2</sup>

### ABSTRACT

Hemoglobin (Hb) released into the circulation during hemolysis and chemically modified Hb proposed for use as oxygen therapeutics exert toxic effects that are partially attributable to heme's oxidant activity. Native extracellular Hb is scavenged by haptoglobin (Hp) after  $\alpha\beta$ -subunit dimerization. In the absence of Hp, monocyte/macrophage cell-surface CD163 binds and clears Hb. We evaluated several chemically modified Hbs to establish the role of chemical cross-linking patterns and molecular sizes on binding and clearance by each pathway. We found that Hbs possessing  $\beta$ -globin cross-linking, irrespective of polymerization, demonstrate increased Hp affinity compared with  $\alpha$ -globin-stabilized Hbs. These data suggest that Hb  $\alpha$ -subunit accessibility is critical for Hp binding in the absence of dimerization.  $\beta$ -Globin chain cross-linked tetramers/polymers displayed strong polyvalent Hp binding with increased viscosity and formation of visible gel matrices. Modified Hb interaction with CD163 and cellular uptake demonstrated an inverse relation with molecular size, irrespective of  $\alpha$  and  $\beta$  cross-linking. These findings were confirmed by HO-1 induction and intracellular ferritin accumulation in CD163-expressing HEK293 cells. Based on these results, a rational and systematic approach to HBOC design may be used to optimize interaction with endogenous Hb clearance and detoxification pathways. *Antioxid. Redox Signal.* 10, 1449–1462.

### INTRODUCTION

**D**ETOXIFICATION and clearance of extracellular Hb from the circulation has been described to occur through a plasma protein-binding pathway in which Hb  $\alpha\beta$  dimers initially bind to haptoglobin (Hp). Subsequently, the circulating Hb-Hp complex is recognized by the monocyte/macrophage scavenger receptor CD163 and cleared by endocytosis (16, 30). The plasma Hp-binding capacity can be saturated during circumstances of severe hemolysis when Hb exceeds the normal range of circulating Hp concentrations (0.45–3 mg/ml) (16). In circumstance of Hp depletion, an efficient pathway of Hb clearance appears to be functional, as demonstrated in Hp-knockout mice (17) and in humans with anhaptoalbuminemia. Macrophage Hb uptake in

the absence of Hp involves a low-affinity binding site on CD163, which allows efficient Hb endocytosis in cases of high extracellular Hb concentrations (33). Beyond the scenario of severe hemolysis, this pathway is presumed to be operational after red blood cell extravasation and lysis, such as during inflammation and tissue injury (31).

The interactions between Hb and Hp and between Hb and macrophage cell surface CD163 are each influenced independently by unique physical and chemical properties of Hb. In the case of Hp binding, specific amino acid regions within the Hb  $\alpha$ - and  $\beta$ -globin chains have been reported to be critical (14, 15, 19, 39). Whereas these studies delineate the specificity of amino acid regions within each globin chain necessary for Hp interaction, the dominant recognition site(s) remain undefined.

<sup>1</sup>Laboratory of Biochemistry and Vascular Biology, Division of Hematology, Center for Biologics Evaluation and Research (CBER), U.S. Food and Drug Administration (FDA), Rockville, Maryland.

<sup>2</sup>Medical Clinic Research Unit, University of Zurich, and <sup>3</sup>Polymer Physics, Department of Materials, ETH Zurich, Switzerland.

In the case of Hp-independent Hb uptake by cell-surface CD163, the specificity for receptor interaction is contained exclusively within the  $\beta$ -globin chain (33).

Hemoglobin-based oxygen carriers (HBOCs) have been proposed for a range of conditions, including surgical anemia, traumatic blood loss, ischemic events, sickle cell disease, and as broad-scale substitutes for blood in the absence of a safe blood supply. However, clinical advancement in these areas has been slowed by significant adverse-event profiles associated with several HBOCs (38). A critical and often overlooked concept in the development of HBOCs is that each disease state requires differing durations of HBOC exposure to achieve a desired therapeutic effect with minimal or no toxicity. Therefore, optimizing exposure-response relations for specific disease states by considering the endogenous mechanisms of Hb clearance in HBOC design may enhance efficacy and safety. Relevant to this concept is that candidate patients targeted for HBOC therapies often experience one or several concomitant conditions such as: tissue injury, inflammation, collagen and vascular disorders, infection, and glucocorticoid treatment. In each condition, Hp and monocyte/macrophage cell-surface CD163 may be increased in the short term (21, 36).

In general, chemical or recombinant modification to hemoglobin (Hb) or both impart structural constraints within the central cavity or on the surface of the protein or both. Ultimately, modifications to Hb are directly translated to the heme prosthetic groups and redefine native Hb oxygen affinity and cooperativity. Similarly, the toxicity associated with both native extracellular and Hb subjected to modification can also be traced back to the heme prosthetic groups (9, 12, 24). In the absence of intraerythrocytic biochemical and physical protective mechanisms, Hb may be subjected to prooxidative as well as nitrosylative/nitrosative processes, which typically result in vasoconstriction, inflammation, and ultimately, tissue injury (8, 20).

Administration of HBOCs represents a unique circumstance during which Hb exposure can exceed even the most severe cases of hemolytic anemia. Interactions with one or both of the endogenous Hb-scavenger pathways could thus critically influence the toxicity profile of specific HBOCs. Typically, chemical modification to native human or animal source Hb generates individual HBOCs with either  $\alpha\alpha$ - or  $\beta\beta$ -globin chain intramolecular cross-linking. Additional protein surface modifications include polymerization or surface conjugation or both. Intra- and intermolecular modification of Hb in the case of HBOCs protects against dimer formation and extends circulating half-life, respectively. Although much research has been performed to understand altered oxygen transport/delivery properties, as well as detoxification processes focused on modulation of NO, the specific consequences of structural Hb modifications on the interaction with the endogenous Hb-scavenging pathways have not yet been investigated.

In the current study, we evaluated several HBOCs with differing intra- and intermolecular modifications on the interaction with either the plasma protein-binding pathway (Hp) or the cell surface-receptor pathway (cell surface CD163). By using  $\alpha\alpha$  versus  $\beta\beta$  cross-linking pattern and molecular size as structural determinants, we suggest a simple model that might predict functional properties of HBOCs related to preferential interactions with each of the two scavenger systems. Based on these results, a rational and systematic approach to HBOC de-

sign may be used to optimize efficacy and limit toxicity by accounting for existing mechanisms of endogenous Hb-clearance and detoxification pathways.

## MATERIALS AND METHODS

### *Hemoglobin and haptoglobin substances*

Several chemically modified Hbs were used in this study. The nature, subunit-specific chemical modification, and commercial and current abbreviations used in this study are indicated: (a) highly purified Hb (HbA<sub>0</sub>) and (b) oxidized raffinose polymerized HbA<sub>0</sub> (Hemolink;  $\beta$ PolyHb A<sub>0</sub>) was obtained from Hemosol (Mississauga, Ontario, Canada), (c) bis(3,5-dibromosalicyl)fumarate cross-linked human Hb between  $\alpha$ -globin ( $\alpha$ DBBF;  $\alpha$ XLHb), and (d)  $\beta$ -globin chains ( $\beta$ DBBF;  $\beta$ XLHb) was provided by the United States Army (Washington, DC); (e) the polyethylene glycol (PEG) polymerized and conjugated form of bis(3,5-dibromosalicyl)fumarate cross-linked human Hb  $\alpha$ -globin chains (Poly DCLHb;  $\alpha$ PolyXLHb) was provided by Baxter Healthcare (Deerfield, IL), (f) benzene tetracarboxylate substituted dextran Hb ( $\beta$ DxHb) was provided by Patrick Menu (University Henri Poincaré-Nancy, France); and (g) Oxyglobin ( $\alpha$ PolyBvHb) was purchased from Biopure (Cambridge, MA). Haptoglobin 1-1 and 2-2 was purchased from Sigma Chemical (St. Louis, MO).

### *Size-exclusion chromatography (molecular size distribution)*

HBOC samples (50  $\mu$ l) were evaluated by size-exclusion chromatography (SEC) to compare the molecular size distribution of tetramer, multitetramer, and surface conjugated components. Samples were run on a BioSep-SEC-S3000 (600  $\times$  7.5 mm) SEC column (Phenomenex, Torrance, CA) attached to a Waters 626 pump and Waters 2487 dual-wavelength detector, controlled by a Waters 600s controller using Millenium32 software (Waters Corp., Milford, MA). The running buffer consisted of 0.1 M NaH<sub>2</sub>PO<sub>4</sub>, pH 6.5, pumped at rate of 0.5 ml/min, and the absorbance was monitored at 405 nm. Molecular-size ranges were previously determined by SEC coupled to multi-angle laser light scattering (Wyatt Technology Corp., Santa Barbara, CA).

### *Fractionation and purification of polymerized Hb*

The heterogeneous mixtures making up  $\beta$ PolyHbA<sub>0</sub> and  $\alpha$ PolyBvHb were separated into six and four individual fractions, respectively. The mixture of components making up  $\beta$ PolyHbA<sub>0</sub> and  $\alpha$ PolyBvHb were separated on a Biosep SEC 3000 (600  $\times$  7.5 mm) size-exclusion HPLC column (Phenomenex) attached to a Waters 626 pump and Waters 2487 dual-wavelength detector, controlled by a Waters 600s controller by using Millenium32 software (Waters Corp.). The running buffer consisted of 0.1 M NaH<sub>2</sub>PO<sub>4</sub>, pH 6.5, pumped at rate of 0.5 ml/min, and the absorbance was monitored at 405 nm. Distinct peaks in the chromatogram were collected by using a CF-1 fraction collector (Spectrum Laboratories, Roncho

Dominquez, CA) and further refined to homogeneity. Collected fractions were chromatographed individually by using size-exclusion chromatography and recollected twice after the initial separation and collection. Isolated fractions were buffer exchanged with five 10-ml volumes of 0.9% NaCl and concentrated by using Centricon YM-30 centrifuge tubes (Millipore, Bedford, MA). Fractions molecular sizes and polydispersity were evaluated by using SEC coupled to multiangle laser light-scattering (SEC-MALLS). SEC-MALLS data were acquired and analyzed by using a Wyatt Technology Corp. Dawn-DSP with Astra version 4.73.04 software. The 100- $\mu$ l sample volumes were injected and separated on a Shodex OHPAK SB-806HQ column (300  $\times$  8 mm). The mobile phase consisted of 50 mM sodium phosphate, pH 6.9, pumped at a rate of 0.5 ml/min. For MALLS, samples were run through a dawn DSP laser photometer. The samples then passed through an Optilab DSP interferometric refractometer to determine concentration. Each detector was set to a wavelength of 633 nm.

#### *MALDI-MS (globin chain cross-linking determination)*

HBOC samples (10  $\mu$ l) were desalted by using C18 ZipTips (Millipore) according to the manufacturer's instructions. A 1- $\mu$ l aliquot was pipetted onto a stainless-steel MALDI-MS sample plate and mixed with 1  $\mu$ l of 3,5-dimethoxy-4-hydroxycinnamic acid (sinapinic acid) (Sigma Chemical Co.) saturated in 50% acetonitrile (AcCN)/0.1% trifluoroacetic acid (TFA). The sample/matrix was air dried and analyzed on a PerSeptive Biosystems DERP MALDI-TOF mass spectrometer calibrated manually with purified human serum albumin (Sigma Chemical Co.) and by using Voyager 5.1 software with Data Explorer (Applied Biosystems, Framingham, MA) operated in linear mode.

#### *Surface plasmon resonance (SPR) analysis*

Surface plasmon resonance (SPR) analyses [for review, see (26)] were performed by using a Biacore 3000 instrument (GE Healthcare, Biacore AB, Uppsala, Sweden). For all ligands, CM5 Biacore sensor chips were activated with a 1:1 mixture of EDC/NHS for 7 min. The analyses were carried out by using conditions described previously for Hb and Hp binding (2, 16). Haptoglobin 1-1 was diluted to 5  $\mu$ g/ml in 10 mM sodium acetate, pH 4.5, and immobilized on the CM5 chip at a density of 200 RU. Haptoglobin 2-2 was diluted to 7.5  $\mu$ g/ml in 10 mM sodium acetate, pH 4.5, and immobilized at a density of 300 RU. CD163 was diluted to 50  $\mu$ g/ml in 10 mM sodium acetate, pH 4.0, and immobilized on the CM5 chip to a density of 6,500 RU. The remaining binding sites were blocked with 1 M ethanolamine, pH 8.2, for 7 min. The flow rate for activation, immobilization, and blocking was 5  $\mu$ l/min. A reference cell was made by performing the activation and blocking procedure only. Samples were diluted in the corresponding running buffer for the ligand. The running buffer for haptoglobin 1-1 and haptoglobin 2-2 was HBS-EP (0.01 M Hepes, pH 7.4, 0.15 M NaCl, 3 mM EDTA, 0.005% vol/vol Surfactant P20). For CD163, the running buffer was HBS-P (0.01 M Hepes, pH 7.4, 0.15 M NaCl, 0.005% vol/vol Surfactant P20) with 5 mM  $\text{CaCl}_2$ . All samples were injected at a flow rate of 30  $\mu$ l/min for 5 min and analyzed for 15 min dissociation time. For HP1-1, regeneration of the sensor chip after each anal-

ysis cycle was performed with two 60-s injections of 10 mM glycine-HCl, pH 1.5. For HP2-2, regeneration was performed with two 30-s injections of 10 mM glycine-HCl, pH 1.75. For CD163, regeneration was performed with one 60-s injection of 1.6 M glycine-HCl buffer, pH 3.0. All regenerations were performed at a flow rate of 50  $\mu$ l/min. The Biacore response was expressed in mass-equivalent response units (RUs) and analyzed with BIAevaluation v4.1 software.

#### *Cell culture*

Human embryonic kidney cells (HEK293; Invitrogen) were cultured in Dulbecco's modified Eagle medium (DMEM; Invitrogen) containing 10% fetal calf serum (FCS; Invitrogen). CD163-transduced cells were produced as described (33) and maintained with 5  $\mu$ g/ml blasticidin (Invitrogen).

#### *Quantification of Hb and Hb-Hp uptake by CD163 expressing HEK293 cells*

Hp phenotype 1-1 (Sigma) was labelled with the Alexa-633 protein-labeling kit (Molecular Probes, Eugene, OR). All uptake assays were performed in cell-culture medium without serum. Fluorescent Hb-Hp complexes were generated by combining Hb and Hp at a 1:1 ratio (wt/wt) 10 min before experimentation. After incubation with fluorescent Hb-Hp (3  $\mu$ g/ml) in the presence of the indicated nonfluorescent competitors for 30 min, the cells were trypsinized and washed 3 times with cold,  $\text{Ca}^{2+}$ -free phosphate-buffered saline (PBS) supplemented with EDTA to remove non-ingested Hb-Hp complexes. Uptake of the fluorescent ligand was then quantified with flow cytometry by using a FACScalibur (BD) equipped with a 633-nm He-Ne laser (32).

For immunofluorescence, cells were grown on sterile, endotoxin-free 12-mm glass coverslips pretreated with poly-D-lysine (Invitrogen). After incubation with Hb preparations, cells were washed, fixed with paraformaldehyde, permeabilized with Triton X-100, and stained with polyclonal rabbit anti-Hb (1:1,000) and Alexa594 conjugated goat anti-rabbit (1:1,000; Molecular Probes) antibodies. We previously confirmed equal reactivity of the polyclonal anti-Hb antibody with all tested HBOCs with Western blot (data not shown). Samples were examined with a Carl Zeiss epifluorescence Axioscope 2 equipped with an AxioCam MR digital camera and Axio Vision software.

#### *Intracellular ferritin*

Cells grown in six-well plates were washed 3 times with PBS and subsequently scraped in PBS. After three freeze-thaw cycles, cells were sonicated for 10 s and centrifuged at 16,000 g for 15 min. Ferritin was determined in the supernatant with an Advia Centaur automated chemiluminescence immunoassay system (Bayer Health Care). In the same lysates, total protein was determined according to the Bradford method.

#### *RNA isolation and quantitative real-time reverse transcription PCR (HO-1)*

Total RNA was isolated by using the QIAgen RNeasy Mini Kit (Qiagen), and a DNase digest was performed. Reverse tran-

scription was performed with oligo(d)T primers and M-MuLV Reverse Transcriptase by using the ProSTAR First Strand Kit (Stratagene, Rotkreuz, Switzerland). HO-1 expression was quantified with the LightCycler real-time PCR system (Roche Diagnostics, Basel, Switzerland) and the Fast Start DNA Master SYBR Green I (Roche Diagnostics), as described previously (33). The primers used for gene-specific amplification were as follows: heme oxygenase 1 (HO-1) forward: 5'-AGGGTGA-TAGAAGAGGCCAAGACT-3'; reverse: 5'-TTCCACCGGA-CAAAG TTCATGGC-3'; glyceraldehyde 3-phosphate dehydrogenase (GAPDH) 5'-AACAGCGA CACCCACTCTC-3', 5'-GGAGGGGAGATTCACTGTGGT-3'. HO-1 mRNA levels were normalized to GAPDH levels for each experimental sample. The final data were expressed as mRNA expression in treated cells relative to the expression level in untreated cells.

### Gel formation/viscosity

The viscoelastic properties of the gels have been characterized in a Couette cell attached to a MCR 300 (Paar Physica, Germany) stress-controlled rheometer. The rotating inner body of the Couette cell has been modified to allow measurements with only 1.5 ml of fluid in a shear gap 0.3 mm wide. The temperature was controlled by a Peltier element to within  $\pm 0.01^\circ\text{C}$ . After loading at  $20^\circ\text{C}$ , the sample was presheared at 1,000/s for 10 s to destroy any structures from loading. Then the sample was left at rest for 6 h to form the gel structure. Two parameters characterize a gel: The shear modulus  $G$  (slope in the initial linear part of a stress/strain plot), its stiffness and the yield stress  $\tau_y$  (when the linear regimen is left), its resistance against rupture. These two parameters were obtained from a stress-ramp test (stress  $0 < \tau < 20$  Pa, with a strain limit of 100 to prevent runaway). For a weak gel, both stress and strain in the linear regimen are at the resolution limit of the rheometer. For weak systems, large amplitudes are required to enhance the measuring signal, but these destroy the gel network. High frequencies are prohibited by the inertia of the tool. The flow behavior of the fluidized gels was subsequently tested in a shear-rate ramp test (shear rate,  $10,000 > \dot{\gamma} > 0.1/\text{s}$ ). With the decreasing shear rate, a regelation of the system can be observed. The viscosity-shear-rate curve approaches a slope of  $-1$  at low rates instead of 0 for a nongelling system. In this test mode, large strains and stresses are applied to the sample. The two tests were repeated at  $37^\circ\text{C}$ , after another 6 h of rest time for regelation. Drying of the sample was prevented by a moistened tissue used as a sealing cover.

## RESULTS

### HBOC structural properties

**Intramolecular cross-linking.** MALDI-MS spectra of HbA<sub>0</sub> demonstrate an  $\alpha$ -globin chain  $[\text{M}+\text{H}]^{1+}$  ion at  $m/z = 15123.17$  and a  $\beta$ -globin chain  $[\text{M}+\text{H}]^{1+}$  ion at  $m/z = 15,863.95$  [Fig. 1A1 & B1]. These ions are identical to the theoretic masses of  $\alpha$ - and  $\beta$ -globin chains for human HbA<sub>0</sub>. The ionization patterns of  $\alpha$ - $\alpha$  cross-linked HBOCs with a loss of the  $\alpha$  globin chain  $[\text{M}+\text{H}]^{1+}$  ion is observed in  $\alpha$ XLHb (Fig.

1A2)  $\alpha$ PolyBvHb (Fig. 1A3) and  $\alpha$ PolyXLHb (Fig. 1A4). Loss of the  $\beta$ -globin chain is observed in  $\beta$ XLHb (Fig. 1B5),  $\beta$ DxHb (Fig. 1B6), and  $\beta$ PolyHbA<sub>0</sub> (Fig. 1B7). These data confirm that  $\beta\beta$  cross-linking of Hbs tetramers leads to internalization of these subunits and subsequent exposure or accessibility of their  $\alpha\alpha$ -subunits counterpart, regardless of the size of Hb. Cross-linking the  $\alpha\alpha$  subunits, conversely, will expose  $\beta\beta$ -subunits to solvent.

**Molecular size.** The molecular size distribution, as determined by analytic size-exclusion chromatography is shown in Fig. 1B. Table 1 indicates molecular size, modifying reagent, and general structural properties of HBOCs evaluated in the present study. Of the seven Hbs evaluated, HbA<sub>0</sub> is tetrameric (64 kDa) and nonchemically or genetically stabilized;  $\alpha$ XLHb and  $\beta$ XLHb are tetrameric Hbs, each stabilized by a bis(3,5-dibromosalicyl)fumarate cross-link between  $\alpha$ - and  $\beta$ -globin chains, respectively. Both  $\alpha$ PolyBvHb and  $\beta$ PolyHbA<sub>0</sub> are heterogeneous mixtures of intramolecularly stabilized tetrameric and multitetrameric Hb fractions. In  $\alpha$ PolyBvHb and  $\beta$ PolyHbA<sub>0</sub> the tetrameric fraction predominates over specific multitetrameric fractions. As a more-extensive evaluation, the two heterogeneous HBOCs were separated into their fractional components to correlate CD163 affinity and uptake with the molecular size of each isolated fraction (see later)  $\beta$ DxHb and  $\alpha$ PolyXLHb possess unique molecular-size characteristics in that they are each void of a tetramer with  $\beta$ DxHb demonstrating a weighted average molecular mass of 300 kDa (13, 25) and  $\alpha$ PolyXLHb demonstrating a weighed average molecular mass of 869 kDa (5). Each of these HBOCs demonstrates elution times beginning at the SEC column void volume, thus indicating that even large-molecular-size species are likely present. The molecular-size distribution of fractionated PolyBvHb and  $\beta$ PolyHbA<sub>0</sub> were collected initially from each mixture and then chromatographed an additional 2 times and collected to refine the fractions. Homogeneity was evaluated with size-exclusion chromatography coupled to laser light scattering (Fig. 2A and B and Table 2).

### HBOC interaction with CD163 and haptoglobin

**Haptoglobin binding.** The role of HBOC chemistries as they influence affinities for binding to Hp (1-1) and (2-2) were determined by surface plasmon resonance analysis. Hb-Hp binding studies are represented as relative binding (Fig. 3A) and clearly show that nonstabilized (HbA<sub>0</sub>) as well as cross-linked and polymerized Hbs bind Hp with varying affinity, irrespective of whether dimerization can occur. Relative binding affinities for individual HBOCs were concentration dependent and displayed the same pattern of affinity to both the Hp 1-1 (Fig. 3B) and Hp 2-2 (Fig. 3C) isoforms. The nearly fourfold lower binding affinity to Hp 2-2 seen with all of Hbs compared with Hp 1-1 is consistent with the low-affinity high-capacity binding properties of the Hp 2-2 isoform. HbA<sub>0</sub>, as expected, demonstrated the greatest affinity for both Hp isoforms, whereas  $\alpha$ PolyXLHb demonstrated no Hp binding at any concentration (0.1–200 nM). The affinity of HBOCs for Hp isoforms followed a distinct pattern of binding that was entirely



**FIG. 1. (A) MALDI-MS showing (A)  $\alpha$ -globin chain cross-linked HBOCs where (1) HbA<sub>0</sub>  $\alpha$ -globin chain ions  $[M+H]^+ = 15,123$   $m/z$  and the  $\beta$ -globin chain ions  $[M+H]^+ = 15,164$   $m/z$ ; (2)  $\alpha$ XLHb ( $\beta$ -globin chains  $[M+H]^+ = 15,864$   $m/z$ ), (3)  $\alpha$ PolyBvHb ( $\beta$ -globin chains  $[M+H]^+ = 16,077 - 16,679$   $m/z$ ); and (4)  $\alpha$ PolyXLHb ( $\beta$ -globin chains  $[M+H]^+ = 15,862$   $m/z$  and PEG  $\beta$ -globin chain conjugates  $[M+H]^+ = 19,227$   $m/z$ ). (B)  $\beta$ -Globin chain cross-linked HBOCs where (1) HbA<sub>0</sub>  $\alpha$ -globin chain ions  $[M+H]^+ = 15,123$   $m/z$  and the  $\beta$ -globin chain ions  $[M+H]^+ = 15,164$   $m/z$ ; (2)  $\beta$ XLHb ( $\alpha$ -globin chains  $[M+H]^+ = 15,123$   $m/z$ ); (3)  $\beta$ DxHb ( $\alpha$ -globin chains  $[M+H]^+ = 15,124$   $m/z$ ); and (4)  $\beta$ PolyHbA<sub>0</sub> ( $\alpha$ -globin chains  $[M+H]^+ = 15,123-15,382$   $m/z$ ). (B) Size-exclusion chromatography of HBOCs fitting into three categories: (A) poly-tetrameric/conjugate (no tetramer), (B) heterogeneous poly-tetrameric + tetrameric, and (C) Tetrameric. Blue,  $\alpha\alpha$ -cross-linked Hbs; red,  $\beta\beta$ -cross-linked Hbs. (For interpretation of the references to color in this figure legend, the reader is referred to the web version of this article at [www.liebertonline.com/ars](http://www.liebertonline.com/ars)).**

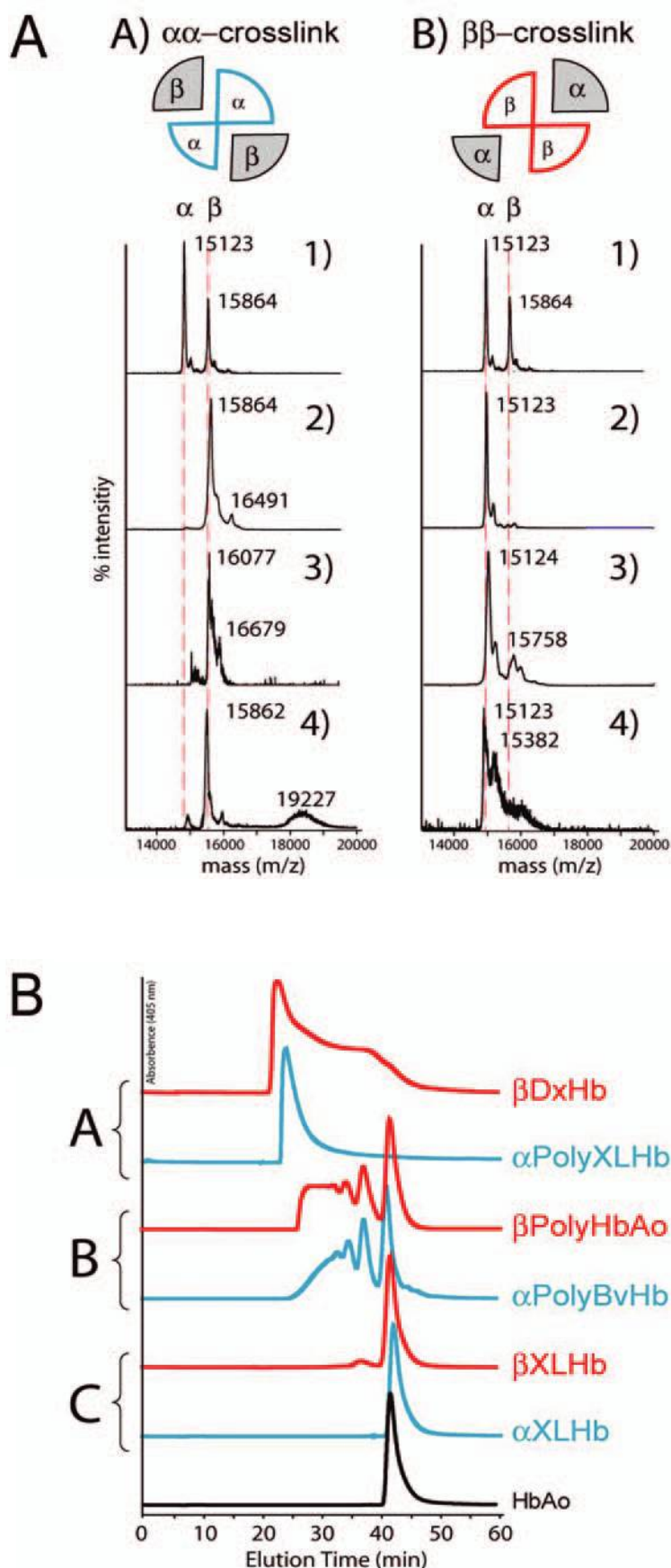

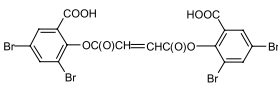

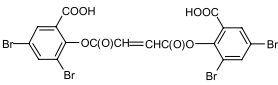

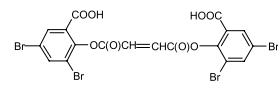
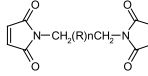
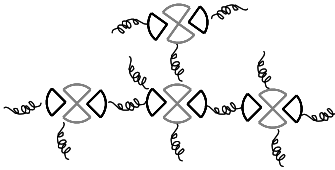
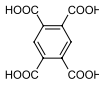
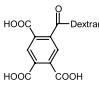
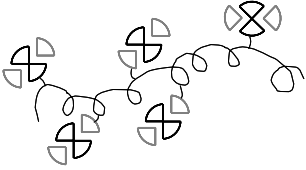
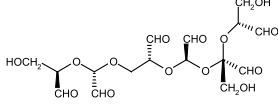
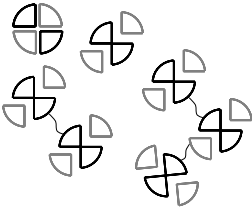
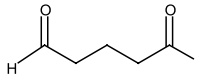
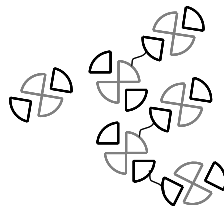
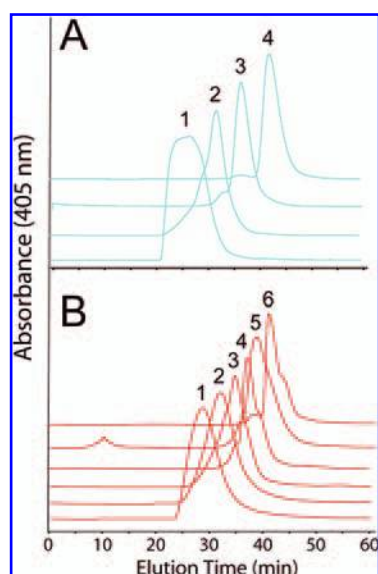


TABLE 1. HBOC GENERAL CHARACTERISTICS

Hemoglobin	Molecular size (kDa)	% Tetramer	Chemical modifier	General structure(s)
HbA0	64–70 (5)	100	None	
$\alpha$ XLHb	64–70 (5)	95 (~5% ditetramer)	 $\alpha\alpha$ - Intermolecular cross-linking	
$\beta$ XLHb	64–70	95\	 $\beta\beta$ - Intermolecular cross-linking	
$\alpha$ PolyXLHb	300–4,000	0	 $\alpha\alpha$ - Intermolecular cross-linking  Surface conjugation/polymerization [R = (CH <sub>2</sub> CH <sub>2</sub> -O-)] $n \sim 40$ -60	
$\beta$ DxHb	300 (25) (64 to >600)	0	 $\beta\beta$ - Intermolecular cross-linking  Surface conjugation/polymerization	
$\beta$ PolyHbA <sub>0</sub>	32 to >600 (~5% dimer/ unstabilized tetramer) (22)	32.7	 $\beta$ Intra/intermolecular cross-linking	
$\alpha$ PolyBvHb	87.2–502.3 (4)	37.2	 $\alpha$ Intra/intermolecular cross-linking	

Molecular sizes are based on size-exclusion chromatography coupled to multiangle laser light scattering, or published studies where indicated. Grey wedges,  $\alpha$ -globin chain; black wedges,  $\beta$ -globin chain; general structures adapted from ref. 27.



**FIG. 2.** Size-exclusion chromatography of purified fractions isolated from the heterogeneous mixtures of (A)  $\alpha$ PolyBvHb and (B)  $\beta$ PolyHbA<sub>0</sub>. Blue,  $\alpha\alpha$ -cross-linked Hbs; red,  $\beta\beta$ -cross-linked Hbs. (For interpretation of the references to color in this figure legend, the reader is referred to the web version of this article at [www.liebertonline.com/ars](http://www.liebertonline.com/ars)).

consistent with intramolecular cross-linking in the following order ( $\text{HbA}_0 > \beta\text{XLHb} = \beta\text{DxHb} > \beta\text{PolyHbA}_0 > \alpha\text{XLHb} = \alpha\text{PolyBvHb} > \alpha\text{PolyXLHb}$ ). The  $\beta\beta$ -cross-linked Hbs demonstrated a 15–30% reduction, whereas the  $\alpha\alpha$ -cross-linked Hbs demonstrated 50–95% reduction in Hp 1-1 binding affinity compared with  $\text{HbA}_0$ . Taken together, these data suggest that an accessible unconstrained  $\alpha$ -globin chain is an important structural feature for Hp interaction when Hb protein dimerization is not possible.

**CD163 interaction.** The Hp-independent interactions of HBOCs with CD163 were evaluated by using surface plasmon resonance analysis to determine Hb relative receptor affinities, and the previously described cell-based endocytotic assay (33) was used to determine the extent of Hb- and HBOC-mediated competition of fluorescent Hb-Hp uptake in CD163-expressing cells. A low-affinity method for direct Hb binding to CD163 has previously been reported by using SPR analysis

(23); however, the competitive cellular endocytosis assay allows a more-specific evaluation of the low-affinity interactions between native Hb and HBOC with the CD163 receptor. Relative binding affinities of each Hb to CD163 and the results of the competitive uptake assay with the different Hbs were evaluated (Fig. 4A and B). Hbs with molecular sizes of  $\sim 64$  kDa (tetramer) bind to CD163 with the highest affinity and, accordingly, were among the most potent inhibitors of Hp-Hb<sub>h</sub> uptake in CD163-expressing cells. Hbs with intermediate CD163 binding affinity,  $\beta\text{PolyHbA}_0$  and  $\alpha\text{PolyBvHb}$ , demonstrated Hb-Hp competition properties similar to those of tetrameric HBOCs—the likely cause being the presence of  $\sim 30$ –40% tetramer in solution. Conversely, the exclusively nontetrameric Hbs,  $\beta\text{DxHb}$  and  $\alpha\text{PolyXLHb}$ , bound to CD163 with the lowest affinity and were minimally taken up by CD163-expressing cells. The order of uptake was as follows:  $\text{HbA}_0 > \alpha\text{XLHb} = \beta\text{XLHb} > \beta\text{PolyHb} = \alpha\text{PolyHbBv} > \text{DxHb} = \alpha\text{PolyXLHb}$ . Further to confirm that the CD163 receptor affinity and cellular-uptake results observed were molecular size dependent, the two heterogeneous-molecular-size HBOCs ( $\alpha\text{PolyBvHb}$  and  $\beta\text{PolyHbA}_0$ ) were fractionated (see Fig. 2 and Table 2), and individual fractions were then evaluated in the competition assay. This allowed molecular-size comparison while controlling for the chemical modifier. Four and six distinct fractions were collected from  $\alpha\text{PolyBvHb}$  and  $\beta\text{PolyHbA}_0$  mixtures, respectively. Fractions ranged in molecular size from 32 kDa ( $<5\%$  in each Hb mixture) to 400 kDa ( $\alpha\text{PolyBvHb}$ ) and  $>600$  kDa ( $\beta\text{PolyHbA}_0$ ). Each fraction in  $\beta\text{PolyHbA}_0$  and  $\alpha\text{PolyBvHb}$  demonstrates a concentration-dependent inhibition of Hp-Hb<sub>h</sub> cellular uptake (Fig. 5A and B). Similar to the nontetramer containing Hbs, the largest molecular-size fractions demonstrate the least Hp-Hb<sub>h</sub> uptake inhibition. The range of molecular sizes from all chemically modified Hbs confirms a highly correlated ( $r^2 = 0.80$ ) inverse relation between molecular size and uptake competition (Fig. 5C), which was (as opposed to Hp binding) not related to the globin chain involvement in intramolecular cross-linking ( $\alpha\alpha$  vs.  $\beta\beta$ ). This model may be applied in the design of new HBOCs site-specifically modified with structural features to facilitate enhanced or impeded removal by these pathways. In all binding and cellular-uptake experiments, serum/plasma-free buffers and media were used. The influence of serum and plasma components in these studies would have confounded results, likely by increasing Hp or soluble CD163 concentrations.

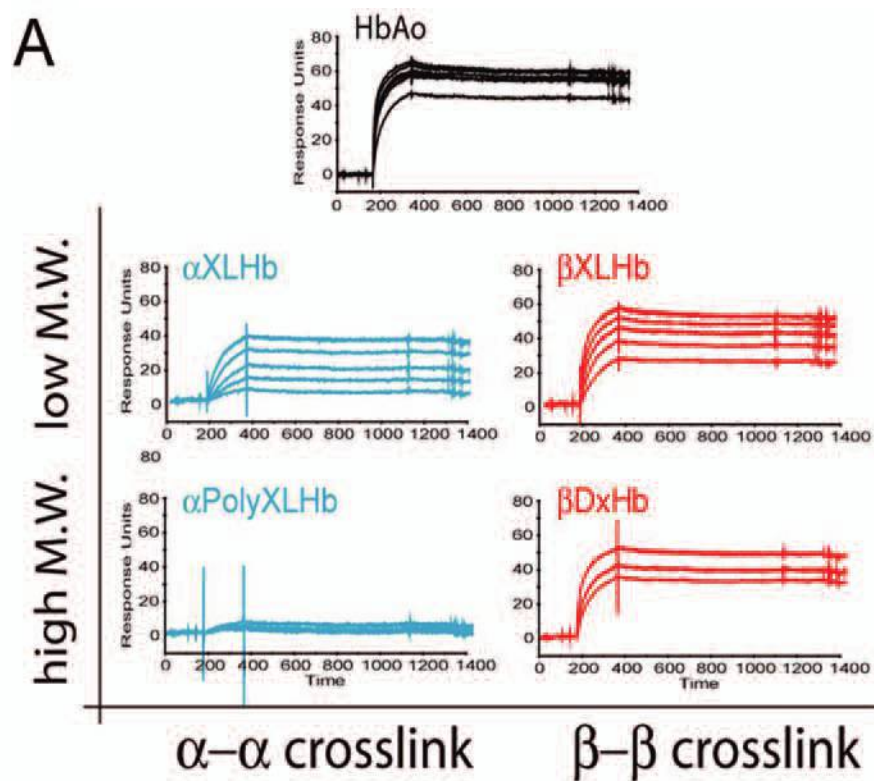
TABLE 2. HBOC COLLECTED FRACTION CHARACTERISTICS

$\alpha\text{PolyBvHb}(4)$	$M_n$ (kDa)	$M_w$ (kDa)	$M_w/M_n$	Tetramer replicate	$\beta\text{PolyHbA}_0$	$M_n$ (kDa)	$M_w$ (kDa)	$M_w/M_n$	Tetramer replicate
Fraction 1	491.5	502.3	1.022	4–6	Fraction 1	$\geq 600^a$	$\geq 600^a$	—	$\geq 8$
Fraction 2	271.3	272.4	1.007	3	Fraction 1	450	450	1.00	6
Fraction 3	184.4	185.9	1.008	2	Fraction 3	220	220	1.00	3
Fraction 4	86.5	87.2	1.008	1	Fraction 4	150	150	1.00	2
					Fraction 5	71.0	71.0	1.00	1
					Fraction 6	32–71 <sup>b</sup>	32–71 <sup>b</sup>	—	0.5–1

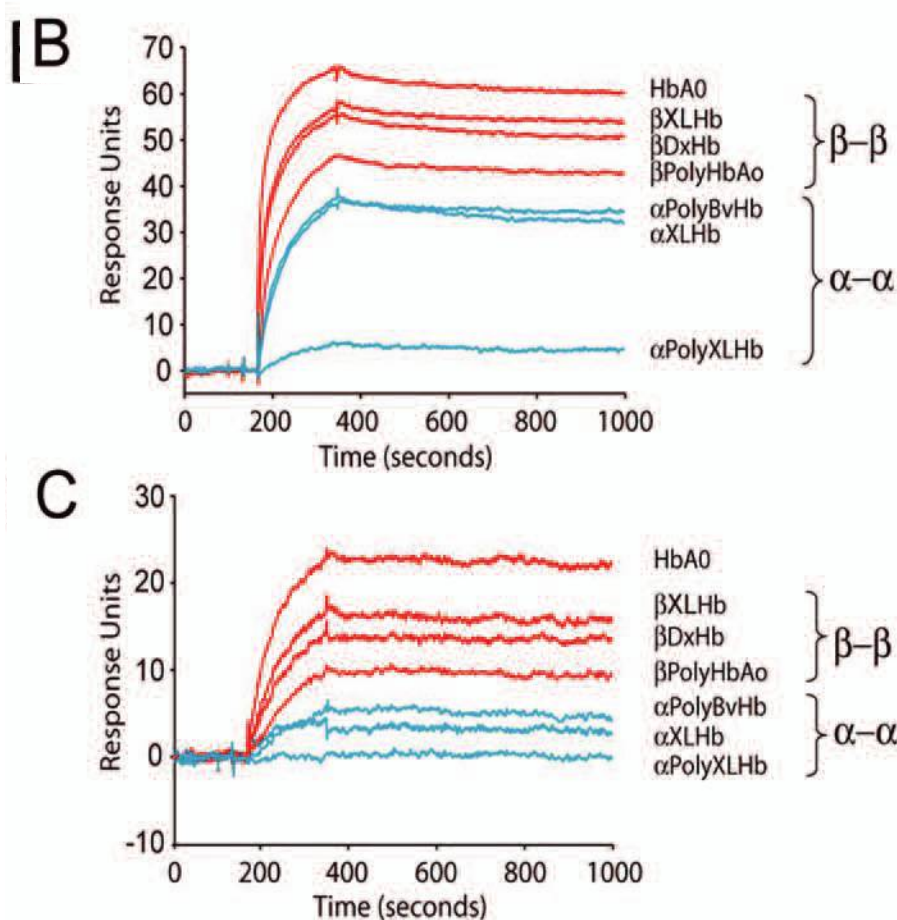
Collected fractions from the initial run were chromatographed and recollected an additional 2 times. Collection occurred at the center of the eluted peak. The initial and tail elution volumes were avoided.

<sup>a</sup>Fractions were collected at elution volumes approaching the Biosep 3000S SEC column void volume (600 kDa).

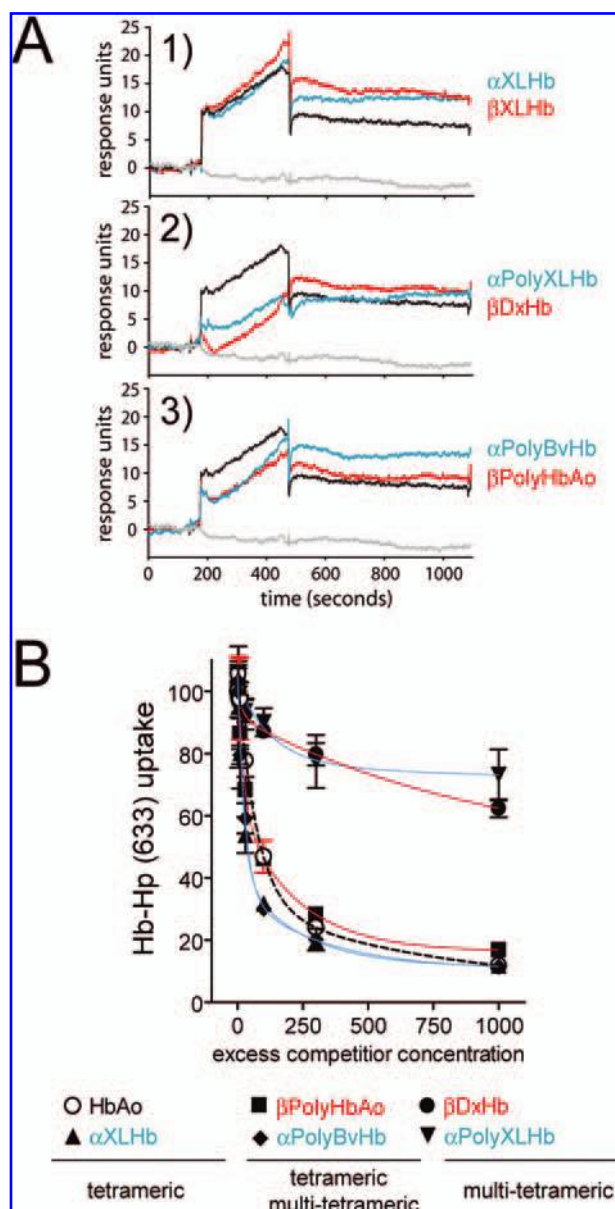
<sup>b</sup>Collection included stabilized and nonstabilized tetramer as well as dimer.



**FIG. 3.** Surface plasmon resonance-binding analysis of stationary phase-bound Hp 1-1 and Hp 2-2 with soluble-phase HBOCs. (A) High and low Hp 1-1 relative-binding-affinity HBOCs at concentrations from 1 to 200 nM heme. (B) Relation in relative Hp 1-1 binding of  $\alpha\alpha$  and  $\beta\beta$  globin cross-linked HBOCs at 200 nM. (C) Relation in relative Hp 2-2 binding of  $\alpha\alpha$  and  $\beta\beta$  globin cross-linked HBOCs at 200 nM. Blue,  $\alpha\alpha$ -cross-linked Hbs; red,  $\beta\beta$ -cross-linked Hbs. (For interpretation of the references to color in this figure legend, the reader is referred to the web version of this article at [www.liebertonline.com/ars](http://www.liebertonline.com/ars)).



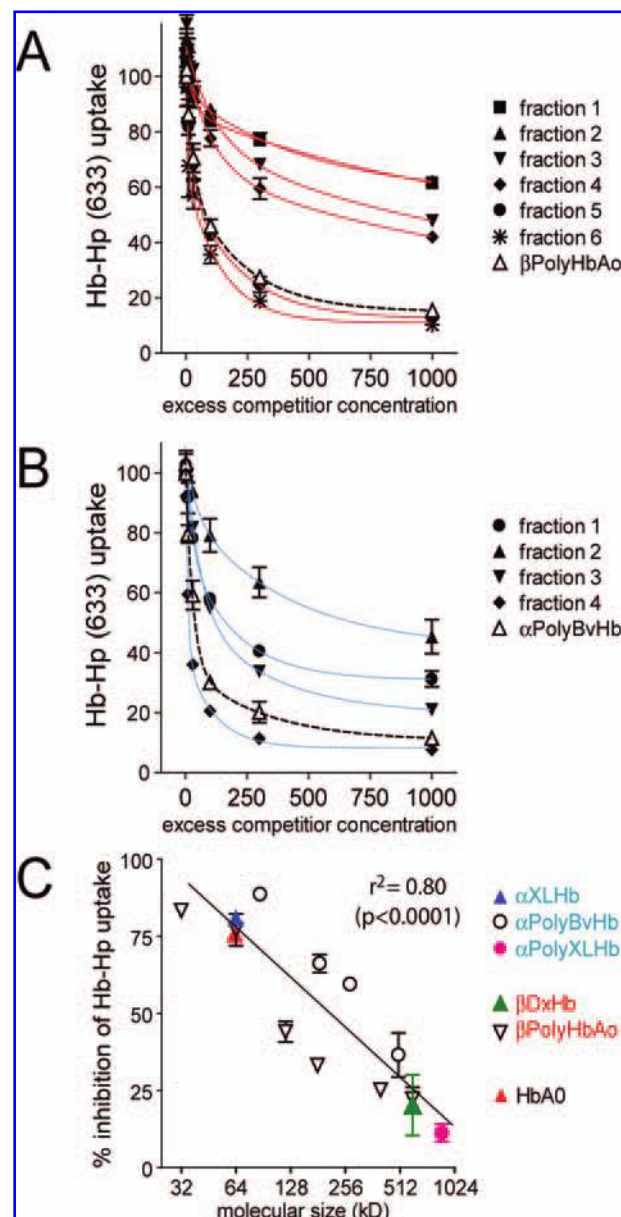




**FIG. 4. Relation between CD163-receptor affinity and competitive uptake inhibition of fluorescently labeled Hb-Hp complex.** (A) Surface plasmon resonance-binding analysis of stationary phase-bound CD163 with soluble-phase HBOCs at 10  $\mu$ M. (1) tetrameric: HbA<sub>0</sub> (black),  $\alpha$ XLHb (blue),  $\beta$ XLHb (red); (2) multitetrameric:  $\beta$ DxHb (red),  $\alpha$ PolyXLHbA<sub>0</sub> (blue); and (3) tetrameric + multitetrameric:  $\beta$ PolyHbA<sub>0</sub> (red),  $\alpha$ PolyBvHb (blue). Buffer (10 mM HEPES, 150 mM NaCl, and 0.5 mM CaCl<sub>2</sub>, pH 7.4). (B) Uptake of fluorescent Hb-Hp in the presence of increasing concentrations of nonlabeled HBOCs as competitor (competitor concentrations are given as  $\mu$ M heme). Data are given as percentage fluorescent signal relative to Hb-Hp uptake in the absence of any competitor and indicate mean  $\pm$  SD of three experiments. Blue,  $\alpha\alpha$ -cross-linked Hbs; red,  $\beta\beta$ -cross-linked Hbs. Grey line, running buffer 10 mM HEPES, 150 mM NaCl, and 0.5 mM CaCl<sub>2</sub>, pH 7.4. (For interpretation of the references to color in this figure legend, the reader is referred to the web version of this article at [www.liebertonline.com/ars](http://www.liebertonline.com/ars)).

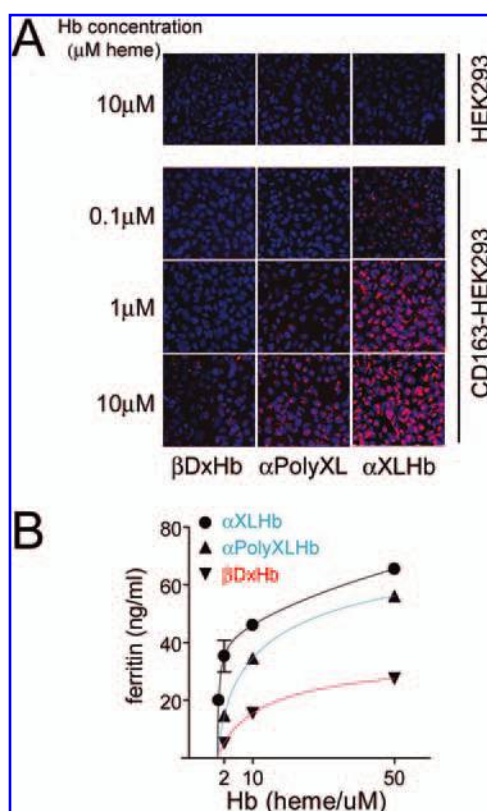
### HBOC biologic and biophysical properties

**Endocytosis and ferritin induction in CD163-HEK cells.** To explore whether differences in HBOC interactions with the Hb scavenger receptor results in different endocytosis by CD163 expressing cells, we compared the cellular uptake of

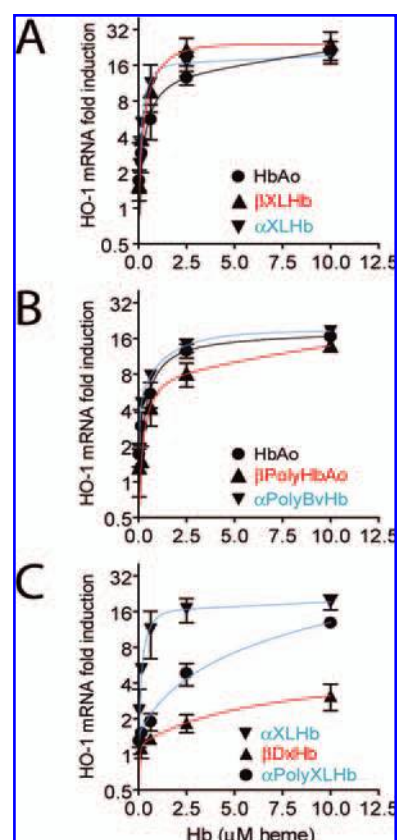


**FIG. 5. Uptake of fluorescent Hb-Hp in the presence of increasing concentrations of nonlabeled HBOCs as competitor (competitor concentrations are given as  $\mu$ M heme).** Data are given as percentage fluorescent signal relative to Hb-Hp uptake in the absence of any competitor and indicate mean  $\pm$  SD of three experiments. (A) The competitors represent individual fractions of  $\beta$ PolyHbA<sub>0</sub> (1, largest molecular size; 6, smallest molecular size), whereas in (B), the competitors represent individual fractions of  $\alpha$ PolyBvHb (1, largest molecular size; 4, smallest molecular size). C: Relation between molecular size of individual HBOCs and size-defined fractions thereof with fluorescent Hb-Hp uptake in the presence of a 100-fold excess concentration of the respective Hb preparation. (For interpretation of the references to color in this figure legend, the reader is referred to the web version of this article at [www.liebertonline.com/ars](http://www.liebertonline.com/ars)).

tetrameric  $\alpha$ XLHb with two multitetrameric HBOCs ( $\beta$ DxHb and  $\alpha$ PolyXLHb) by CD163-expressing HEK293 cells (CD163-HEK cells). Incubation of CD163-HEK cells with equal concentrations of  $\beta$ DxHb and  $\alpha$ PolyXLHb for 60 min resulted in a considerably lesser amount of intracellular immunoreactive Hb than was observed after incubation with  $\alpha$ XLHb (Fig. 6A). No difference was observed when comparing CD163-mediated uptake of  $\alpha\alpha$ - and  $\beta\beta$ -cross-linked tetrameric Hb (data not shown). To confirm that the differences in immunostaining are indeed a result of reduced intracellular Hb and not due to altered antibody reactivity, we demonstrated identical antibody reactivity for all three HBOCs by Western blot (not shown). Accordingly, treatment of CD163-HEK cells with  $\beta$ DxHb and  $\alpha$ PolyXLHb resulted in a markedly reduced intracellular accumulation of ferritin after 12 h (Fig. 6B). Compatible with lower CD163-receptor-binding affinities of  $\beta$ DxHb and  $\alpha$ PolyXLHb, the differences in uptake and ferritin accumulation were most pronounced at the lower Hb concentrations tested (*i.e.*, 2  $\mu$ M).



**FIG. 6.** (A) CD163-expressing HEK293 cells were incubated for 30 min with the indicated concentrations of a tetrameric Hb ( $\alpha$ XLHb) and two different polymeric Hbs ( $\beta$ DxHb and  $\alpha$ PolyXLHb). After 30 min, cells were washed and stained with a polyclonal antibody to human Hb. Compared with the tetrameric Hb, considerably less uptake could be observed after incubation with equal concentrations of either polymeric Hb. No Hb uptake could be observed into CD163-negative cells (*top*). (B) CD163-HEK293 cells were incubated with the indicated tetrameric and large polymeric Hbs, and intracellular ferritin concentrations were determined after 12 h.



**FIG. 7.** CD163-HEK293 cells were incubated with the indicated HBOCs for 8 h, and HO-1 mRNA expression was determined by real-time PCR. (A) Tetrameric HBOCs:  $\alpha$ XLHb (blue),  $\beta$ XLHb (red). (B) Tetrameric + multitetrameric:  $\beta$ PolyHbA<sub>0</sub> (red),  $\alpha$ PolyBvHb (blue). (C) Multitetrameric:  $\beta$ DxHb (red),  $\alpha$ PolyXLHbA<sub>0</sub> (blue). In (A) and (B), values for non-cross-linked HbAo are given for comparison. HO-1 mRNA levels are corrected for changes in GAPDH levels and are given as fold expression relative to the mRNA level of nontreated cells. Data represent mean  $\pm$  SD of three experiments.

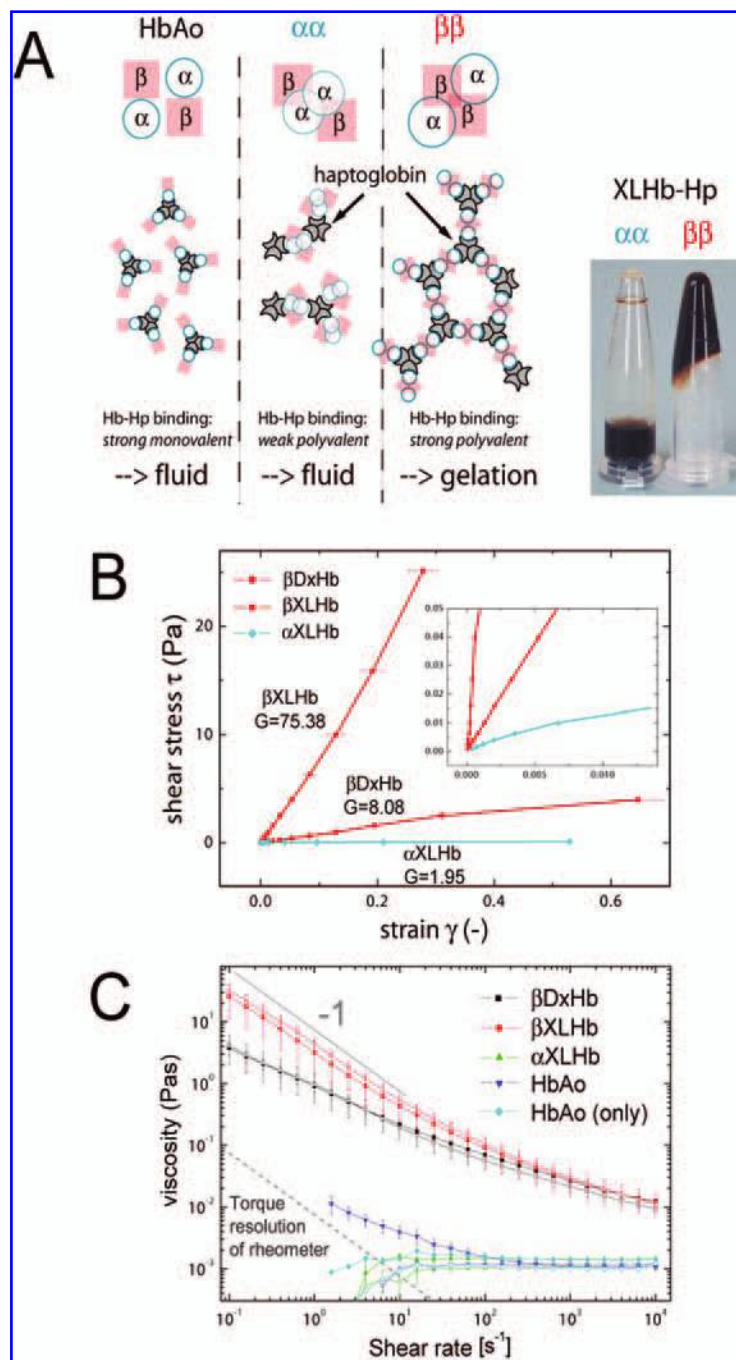
**HO-1 induction in CD163-HEK cells.** We recently described that increased expression of the inducible heme-breakdown enzyme heme oxygenase (HO-1) is the principle cellular response to CD163-mediated Hb endocytosis (29). We thus compared HO-1 mRNA induction by different HBOCs in CD163-HEK cells. Although the tetrameric (Fig. 6A) and mixed tetrameric/multitetrameric (Fig. 6B) molecular-size HBOCs all induced comparable HO-1 mRNA after 8 h, the dose-dependent HO-1 induction was considerably less for the multitetrameric molecular-size HBOCs, which display low CD163 interaction and minimal CD163-mediated endocytosis ( $\beta$ DxHb and  $\alpha$ PolyXLHb (Fig. 7C). Lower HO-1 induction by large-molecular-size modification of Hb was most pronounced at low extracellular Hb-heme concentrations (1–2  $\mu$ M), an observation that is compatible with the low CD163-binding affinity of these molecules. Only minimal HO-1 mRNA induction was induced by all HBOCs in CD163-negative HEK293 cells (data not shown).



**Polyvalent high-affinity Hb-Hp interaction results in the formation of Hb-Hp gels.** We hypothesized that polymerization of Hb under conditions that preserve Hp binding could result in polyvalent Hp-binding molecules. Hp contains two (Hp 1-1 phenotype) or more (Hp 2-2) Hb-binding sites, which allow the formation of large three-dimensional HBOC-Hp macromolecular assemblies (Fig. 8A). Compatible with this model, we performed a rheologic analysis of equimolar mixtures of tetrameric or polymeric HBOCs with Hp (mixed phenotype), which revealed biophysical properties compatible with the formation of three-dimensional macromolecular gel structures in case of  $\beta\beta$  cross-linked Hbs. In contrast, Hb-Hp

complexes including native HbA<sub>0</sub> (a monovalent Hp-binding molecule in its dimeric form) displayed pure fluid characteristics with no detectable gelation, indicating the importance of the unique structural properties of certain HBOCs as polyvalent Hp-binding molecules. With rheologic assessment of shear stress-strain relations (Fig. 8B), we found that the strong Hp interaction with  $\beta\beta$  cross-linked HBOCs ( $\beta$ XLHb and  $\beta$ DxHb) was associated with the formation of much stronger/less deformable macromolecular structures, compared with the weak Hp binding of  $\alpha\alpha$  cross-linked HBOCs ( $\alpha$ XLHb). The strong polyvalent intramolecular interactions in  $\beta\beta$  cross-linked HBOCs result in the buildup of large three-dimensional macro-

**FIG. 8. (A) Proposed model of the putative multimeric Hp binding of  $\beta\beta$  cross-linked Hb, which is expected to result in the buildup of three-dimensional gel-like structures.** Monovalent Hp interaction with HbA<sub>0</sub> shows that binding is terminated at the  $\alpha$ -globin chain interaction of the  $\alpha$ - $\beta$  dimer. The same is true for nondissociable  $\alpha\alpha$  cross-linked Hb, because only weak interaction occurs with a free  $\beta$ -globin chain. In the case of nondissociable  $\beta\beta$  cross-linked Hb, a strong interaction occurs with the free  $\alpha$ -globin chain, and the additional  $\alpha$ -globin chain can interact with another Hp. Over time, Hp and  $\beta\beta$  cross-linked Hb forms a nonterminating chain or matrix. **(B)** The strain-shear-stress relation shows a much higher deformability of  $\alpha$ XLHb-Hp (blue) compared with both  $\beta$ -cross-linked Hbs ( $\beta$ XLHb-Hp and  $\beta$ DxHb-Hp, red) at any given shear stress.  $G$ , The shear-stress modulus, which is a quantitative measure of the gel stiffness (defined as the slope in the initial linear part of a stress/strain plot, shown in the insert). **(C)** The shear rate-viscosity relation. Compatible with the formation of gel-like macromolecular assemblies, higher viscosity is measured in mixtures of Hp with the two  $\beta$ -cross-linked Hbs ( $\beta$ XLHb-Hp and  $\beta$ DxHb-Hp). As is characteristic for gel structures, the viscosity increases at low shear rates, but even at very high shear rates, the viscosity remained increased compared with the nongelating Hb-Hp mixtures. The changes in viscosity at high and low shear-stress rates reproducibly vary with both increasing and decreasing shear-stress rates. This indicates a reversible cycle of primary gelation-gel disruption (at high shear rate) and subsequent regelation (at decreasing shear rate). In contrast, only minimal differences were found in the measured viscosity between mixtures of Hp with either  $\alpha$ XLHb or HbA<sub>0</sub> or HbA<sub>0</sub> alone (without Hp). In the absence of Hp, no differences in viscoelastic properties were seen among all HBOCs tested. (Data are presented as mean  $\pm$  SD of three measurements; open symbols, measurements at 37°C; solid symbols, measurements at 20°C).



molecular assemblies, visible to the observer as the formation of solid gels (Fig. 8A, inset). The very weak gelation characteristics within  $\alpha$ XLHb mixtures result in a small yield stress and did not result in visible gel formation. Interestingly, gel formation after mixing equimolar concentrations of Hp with  $\beta$ XLHb was considerably slower (several hours) compared with the immediate gel formation observed on mixing  $\beta$ DxHb with Hp (Fig. 8C). The different kinetics in the buildup of stable macromolecular assemblies for these two  $\beta\beta$  cross-linked HBOCs may be related to the higher number of putative Hp-binding sites within the highly polymerized DxHb.

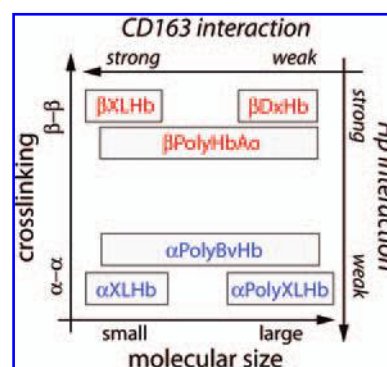
## DISCUSSION

HBOCs, also known as “blood substitutes,” display a diversity of intra- and intermolecular cross-linking as well as molecular sizes, which leads to differences in oxygen affinity and redox reaction properties. These diverse physicochemical characteristics likely translate to differing physiologic responses, such as hypertension, oxidative toxicity, and clearance mechanisms. In this study, we introduced a novel concept in which a classifiable structure–function relation based on HBOC intra- and intermolecular stabilization can be used to predict HBOC interaction and clearance by established scavenging pathways for circulating extracellular Hb.

Chemical modification of Hb involves intramolecular cross-linking to promote tetramer stabilization and the enhancement of oxygen delivery to tissues. Although not systematically studied, it is known that different cross-linking reagents and reaction conditions (*e.g.*, the initial starting material oxy vs. deoxy Hb) favor modification of either the  $\alpha$ - or  $\beta$ -chains. Increasing the molecular size of Hb *via* chemical conjugation and polymerization is used as a common approach to minimize NO interaction and prolong intravascular retention times.

In the current investigation, by using HPLC and mass spectrometry, we identified with certainty HBOCs that are predominantly cross-linked between either their  $\alpha$ - or  $\beta$ -globin chains and are either exclusively low (tetrameric), high (multitetrameric), or a mixture (tetrameric + multitetrameric) of molecular sizes. We classified these HBOCs according to their ability to interact with the only two known and well-characterized Hb scavenger systems: the plasma-based soluble protein Hp and the monocyte/macrophage-associated scavenger receptor CD163. A surface plasmon-resonance analysis was used to determine relative binding affinities and to rank the extent of interaction between each HBOC and Hp. Similarly, for HBOC interactions with CD163, we additionally used a competitive endocytosis assay, which proved to be highly sensitive to detect the lower-affinity interactions between HBOCs and the cell-surface scavenger receptor.

By mutual integration of structural characteristics and scavenger protein–interaction properties of each HBOC, we were able to derive a model that describes the interaction of HBOCs with Hb-scavenger systems based on cross-linking pattern and molecular size: (a)  $\beta\beta$  cross-linking is associated with higher-affinity binding to Hp than cross-linking between Hb  $\alpha$  chains; (b) increasing the molecular size of an HBOC decreases its interaction with CD163 (Fig. 9). Based on this model, an HBOC affording short exposure at local tissue sites may be achievable



**FIG. 9. Structure–function relation model defining the interaction of HBOCs with endogenous Hb scavenger systems.** HBOCs were structurally classified by molecular size and  $\alpha\alpha$ - vs.  $\beta\beta$ -globin tetramer stabilization and functionally grouped according to their affinity to Hp and CD163, respectively. Whereas the site of tetramer stabilization predicts the affinity to the plasma protein scavenger pathway (Hp), affinity to the macrophage scavenger receptor (CD163) is strongly related to molecular size of HBOCs. Blue,  $\alpha\alpha$ -cross-linked Hbs; red,  $\beta\beta$ -cross-linked Hbs. (For interpretation of the references to color in this figure legend, the reader is referred to the web version of this article at [www.liebertonline.com/ars](http://www.liebertonline.com/ars)).

by creating a smaller-molecular-size HBOC with cross-linking between  $\beta$ -globin chains, thus, favoring clearance by CD163 (small molecular size) and rapid Hp clearance ( $\beta$  cross-linking). If longer exposure times are desired, a large-molecular-size HBOC with internal  $\alpha$  cross-linking would tend to limit local tissue clearance by CD163 and Hp, respectively. Notably, these two structure–function relations appear not to be interrelated, and no specific association with the type of chemistry used to modify Hb seems to be present. An exception to this general observation may be with PEG-based Hb modifications. Several approaches have been used to modify Hb with differing PEG molecules, which either create exclusively tetrameric conjugates (18) or polymer conjugates (10, 11), and each imparts very different physical properties, such as colloid osmotic pressure, viscosity, radius of hydration, and potential for dimerization (35). These differences may lead to differing interactions with Hp, CD163, or potentially other receptors specific for PEG on the surface of macrophages (37). Future work in this area should be conducted, as it will provide valuable insight into local tissue-clearance mechanisms for HBOCs modified with PEG.

Hb dimerization into  $\alpha\beta$  subunits is generally thought to be a requirement for Hp binding. Early observations made before the development of HBOCs demonstrated that intra-globin chain cross-linking of Hb weakened but did not abolish Hp binding. Bis-(*N*-maleimidomethyl)ether  $\beta$ -globin chain cross-linked human Hb was shown to exhibit weak Hp binding that was displaceable by native Hb (6). Later studies showed that tetrameric Hb stabilized between  $\beta$ -globin chains with 2-*nor*-2-formylpyridoxal 5'-phosphate rapidly bound to Hp. The addition of increased concentrations of  $\beta$  globin-stabilized Hb tetramer and Hp led to slow polymerization of the two proteins (3). More recently, *in vivo* studies suggest that distribution and clearance of  $\beta\beta$ -trimesyl cross-linked human Hb is directly influenced by Hp binding when administered at low doses (34).



Unique to these studies is an exclusive use of  $\beta$ -cross-linked Hb tetramers. Our data expand on these observations, with a focus on Hp interactions with HBOCs possessing a wide range of internal and surface modifications. We demonstrate that  $\beta$  cross-linking facilitates more-avid Hp binding than  $\alpha$  cross-linking, regardless of HBOC molecular sizes. This finding confirms that an accessible  $\alpha$ -globin chain is critical for Hp binding when dimerization cannot occur in modified Hb made up of heterogeneous molecular sizes. Additionally, strong polyvalent Hp binding that progresses to gel-matrix formation occurs with tetrameric but also with polymeric  $\beta$  cross-linked HBOCs. Conversely, only minimal polyvalent Hp binding seems to occur with tetrameric and polymeric  $\alpha$  cross-linked HBOCs.

Macrophage endocytosis by CD163 is the only well-characterized cell-surface receptor-related clearance pathway for extracellular Hb and might be the predominant pathway for elimination of extravasated HBOCs from interstitial spaces. CD163-dependent induction of the heme-breakdown enzyme HO-1 and subsequent release of the HO-1 products carbon monoxide, bilirubin, and ferritin is the major response of macrophages to Hb exposure. Based on the well-characterized antiinflammatory and antioxidant properties of the HO-1 products (28), we and others have postulated that activation of the Hb-CD163-HO-1 pathway may constitute an important antioxidant and antiinflammatory mechanism that serves to limit systemic and local Hb toxicity (1, 29). Our data demonstrate that HBOC molecular size exclusively determines CD163 binding and cellular uptake regardless of  $\alpha$  or  $\beta$  intramolecular cross-linking patterns. We show a clear correlation between molecular sizes of HBOC solutions and their component fractions, ranging from 64 to >1,000 kDa (Fig. 4C). These data demonstrate significant CD163 uptake of tetrameric sizes, essentially no uptake with multitetrameric sizes beyond 500 kDa, and moderate uptake of sizes in between. The type of agent used in chemical cross-linking (specific vs. nonspecific) did not appear to influence CD163 binding/cellular uptake of stabilized HBOCs or their component fractions.

The present work defines two novel critical mechanisms for potential toxicity that are directly related to HBOC structure and scavenger-pathway interactions. First, interactions with Hp that facilitate strong polyvalent binding, as observed with polymerized  $\beta$ -globin chain cross-linked HBOCs (e.g.,  $\beta$ DexHb), could conceivably facilitate aggregation/gel matrix formation followed by occlusion and ischemia in localized tissue beds, particularly under low-flow conditions (e.g., during states of circulatory compromise or shock) in which HBOCs are intended to be beneficial. This process would require a microenvironment of elevated Hp levels, which has been reported to occur through elevation of Hp at local sites of inflammation and tissue injury where granulocyte activation might immediately increase local Hp concentrations through release of granule-stored Hp (7, 36). Second, considering the potential proinflammatory and oxidant properties of many HBOCs, the failure of CD163-mediated clearance of large-molecular-size HBOCs together with the low HO-1-inducing capacity of these same agents might contribute to their clinical toxicity by exacerbation of local tissue injury caused by impaired clearance and unimpeded oxidative reactions.

In conclusion, HBOC interactions with endogenous Hb scavenging and detoxification pathways may help to explain some

HBOC-associated clinical toxicities. Definition of HBOC structural properties that influence their interaction with the plasma protein (Hp) and the cell-surface receptor (CD163) pathways allows a rational approach to HBOC design that optimizes exposure and limits toxicity.

## ABBREVIATIONS

$\alpha$ PolyBvHb, glutaraldehyde polymerized bovine Hb-Oxyglobin;  $\alpha$ PolyXLHb, polyethylene glycol (PEG) polymerized and conjugated form of bis(3,5-dibromosalicyl)fumarate cross-linked human Hb  $\alpha$ -globin chains;  $\alpha$ XLHb, bis(3,5-dibromosalicyl)fumarate cross-linked human Hb between  $\alpha$ -globin chains;  $\beta$ DxHb, benzene tetracarboxylate substituted dextran cross-linked and polymerized Hb;  $\beta$ PolyHb A<sub>0</sub>, oxidized raffinose polymerized HbA<sub>0</sub>-Hemolink;  $\beta$ XLHb, bis(3,5-dibromosalicyl)fumarate cross-linked human Hb between  $\beta$ -globin chains; HbA<sub>0</sub>, highly purified Hb; HBOC, hemoglobin-based oxygen carrier; Hp, haptoglobin; SPR, surface plasmon resonance.

## ACKNOWLEDGMENTS

The opinions and assertions contained herein are the scientific views of the authors and are not to be construed as policy of the United States Food and Drug Administration.

## REFERENCES

1. Abraham NG and Drummond G. CD163-Mediated hemoglobin-heme uptake activates macrophage HO-1, providing an antiinflammatory function. *Circ Res* 99: 911–914, 2006.
2. Asleh R, Guetta J, Kalet-Litman S, Miller-Lotan R, and Levy AP. Haptoglobin genotype- and diabetes-dependent differences in iron-mediated oxidative stress in vitro and in vivo. *Circ Res* 96: 435–441, 2005.
3. Benesch RE, Ikeda S, and Benesch R. Reaction of haptoglobin with hemoglobin covalently cross-linked between the alpha beta dimers. *J Biol Chem* 251: 465–470, 1976.
4. Buehler PW, Boykins RA, Jia Y, Norris S, Freedberg DI, and Alayash AI. Structural and functional characterization of glutaraldehyde-polymerized bovine hemoglobin and its isolated fractions. *Analyt Chem* 77: 3466–3478, 2005.
5. Buehler PW, Boykins RA, Norris S, and Alayash AI. Chemical characterization of diaspirin cross-linked hemoglobin polymerized with poly(ethylene glycol). *Analyt Chem* 78: 4634–4641, 2006.
6. Bunn HF. Effect of sulfhydryl reagents on the binding of human hemoglobin to haptoglobin. *J Lab Clin Med* 70: 606–618, 1967.
7. Cid MC, Grant DS, Hoffman GS, Auerbach R, Fauci AS, and Kleinman HK. Identification of haptoglobin as an angiogenic factor in sera from patients with systemic vasculitis. *J Clin Invest* 91: 977–985, 1993.
8. D'Agnillo F and Alayash AI. Redox cycling of diaspirin cross-linked hemoglobin induces G<sub>2</sub>/M arrest and apoptosis in cultured endothelial cells. *Blood* 98: 3315–3323, 2001.
9. Graca-Souza AV, Arruda MA, de Freitas MS, Barja-Fidalgo C, and Oliveira PL. Neutrophil activation by heme: implications for inflammatory processes. *Blood* 99: 4160–4165, 2002.
10. Hai TT, Pereira DE, Nelson DJ, Catarello J, and Srnak A. Surface modification of diaspirin cross-linked hemoglobin (DCLHb) with chondroitin-4-sulfate derivatives: Part 1. *Bioconjug Chem* 11: 705–713, 2000.

11. Hai TT, Pereira DE, Nelson DJ, Srnak A, and Catarello J. Polymerization of diaspirin cross-linked hemoglobin (DCLHb) with water-soluble, nonimmunogenic polyamide cross-linking agents. *Bioconjug Chem* 10: 1013–1020, 1999.
12. Jeney V, Balla J, Yachie A, Varga Z, Vercellotti GM, Eaton JW, and Balla G. Pro-oxidant and cytotoxic effects of circulating heme. *Blood* 100: 879–887, 2002.
13. Jia Y, Wood F, Menu P, Faivre B, Caron A, and Alayash AI. Oxygen binding and oxidation reactions of human hemoglobin conjugated to carboxylate dextran. *Biochim Biophys Acta* 1672: 164–173, 2004.
14. Kazim AL and Atassi MZ. Haemoglobin binding with haptoglobin: localization of the haptoglobin-binding site on the alpha-chain of human haemoglobin. *Biochem J* 197: 507–510, 1981.
15. Kazim AL and Atassi MZ. Haemoglobin binding with haptoglobin: unequivocal demonstration that the beta-chains of human haemoglobin bind to haptoglobin. *Biochem J* 185: 285–287, 1980.
16. Kristiansen M, Graversen JH, Jacobsen C, Sonne O, Hoffman HJ, Law SK, and Moestrup SK. Identification of the haemoglobin scavenger receptor. *Nature* 409: 198–201, 2001.
17. Lim SK, Kim H, Lim SK, bin Ali A, Lim YK, Wang Y, Chong SM, Costantini F, and Baumann H. Increased susceptibility in Hp knockout mice during acute hemolysis. *Blood* 92: 1870–1877, 1998.
18. Manjula BN, Tsai A, Upadhyaya R, Perumalsamy K, Smith PK, Malavalli A, Vandegriff K, Winslow RM, Intaglietta M, Prabhakaran M, Friedman JM, and Acharya AS. Site-specific PEGylation of hemoglobin at Cys-93(beta): correlation between the colligative properties of the PEGylated protein and the length of the conjugated PEG chain. *Bioconjug Chem* 14: 464–472, 2003.
19. McCormick DJ and Atassi MZ. Hemoglobin binding with haptoglobin: delineation of the haptoglobin binding site on the alpha-chain of human hemoglobin. *J Protein Chem* 9: 735–742, 1990.
20. Minneci PC, Deans KJ, Zhi H, Yuen PS, Star RA, Banks SM, Schechter AN, Natanson C, Gladwin MT, and Solomon SB. Hemolysis-associated endothelial dysfunction mediated by accelerated NO inactivation by decompartmentalized oxyhemoglobin. *J Clin Invest* 115: 3409–3417, 2005.
21. Moestrup SK and Moller HJ. CD163: a regulated hemoglobin scavenger receptor with a role in the anti-inflammatory response. *Ann Med* 36: 347–354, 2004.
22. Adamson JG and Moore C. Hemolink, an o-raffinose crosslinked hemoglobin-based oxygen carrier. In: *Blood Substitutes: Principles, Methods, Products and Clinical Trials*, edited by Chang TMS. Basel: Karger, 1998, p. 62–79.
23. Nielsen MJ, Petersen SV, Jacobsen C, Thirup S, Enghild JJ, Graversen JH, and Moestrup SK. A unique loop extension in the serine protease domain of haptoglobin is essential for CD163 recognition of the haptoglobin-hemoglobin complex. *J Biol Chem* 282: 1072–1079, 2007.
24. Porto BN, Alves LS, Fernandez PL, Dutra TP, Figueiredo RT, Graca-Souza AV, and Bozza MT. Heme induces neutrophil migration and reactive oxygen species generation through signaling pathways characteristic of chemotactic receptors. *J Biol Chem* 282: 24430–24436, 2007.
25. Prouchayret F, Fasan G, Grandgeorge M, Vigneron C, Menu P, and Dellacherie E. A potential blood substitute from carboxylic dextran and oxyhemoglobin: I. Preparation, purification and characterization. *Biomater Artif Cells Immobil Biotechnol* 20: 319–322, 1992.
26. Rich RL and Myszkowski DG. Survey of the year 2006 commercial optical biosensor literature. *J Mol Recognit* 20: 300–366, 2007.
27. Riess JG. Oxygen carriers (“blood substitutes”): raison d’être, chemistry, and some physiology. *Chem Rev* 101: 2797–2920, 2001.
28. Ryter SW, Alam J, and Choi AM. Heme oxygenase-1/carbon monoxide: from basic science to therapeutic applications. *Physiol Rev* 86: 583–650, 2006.
29. Schaer CA, Schoedon G, Imhof A, Kurrer MO, and Schaer DJ. Constitutive endocytosis of CD163 mediates hemoglobin-heme uptake and determines the noninflammatory and protective transcriptional response of macrophages to hemoglobin. *Circ Res* 99: 943–950, 2006.
30. Schaer CA, Vallelan F, Imhof A, Schoedon G, and Schaer DJ. CD163-expressing monocytes constitute an endotoxin-sensitive Hb clearance compartment within the vascular system. *J Leukoc Biol* 82: 106–110, 2007.
31. Schaer DJ, Alayash AI, and Buehler PW. Gating the radical hemoglobin to macrophages: the anti-inflammatory role of CD163, a scavenger receptor. *Antioxid Redox Signal* 9: 991–999, 2007.
32. Schaer DJ, Boretti FS, Schoedon G, and Schaffner A. Induction of the CD163-dependent haemoglobin uptake by macrophages as a novel anti-inflammatory action of glucocorticoids. *Br J Haematol* 119: 239–243, 2002.
33. Schaer DJ, Schaer CA, Buehler PW, Boykins RA, Schoedon G, Alayash AI, and Schaffner A. CD163 is the macrophage scavenger receptor for native and chemically modified hemoglobins in the absence of haptoglobin. *Blood* 107: 373–380, 2006.
34. Ship NJ, Toprak A, Lai RP, Tseng E, Kluger R, and Pang KS. Binding of acellular, native and cross-linked human hemoglobins to haptoglobin: enhanced distribution and clearance in the rat. *Am J Physiol* 288: G1301–G1309, 2005.
35. Svergun DI, Ekstrom F, Vandegriff KD, Malavalli A, Baker DA, Nilsson C, and Winslow RM. Solution structure of poly(ethylene) glycol-conjugated hemoglobin revealed by small-angle X-ray scattering: implications for a new oxygen therapeutic. *Biophys J* 94: 173–181, 2008.
36. Theilgaard-Monch K, Jacobsen LC, Nielsen MJ, Rasmussen T, Udby L, Gharib M, Arkwright PD, Gombart AF, Calafat J, Moestrup SK, Porse BT, and Borregaard N. Haptoglobin is synthesized during granulocyte differentiation, stored in specific granules, and released by neutrophils in response to activation. *Blood* 108: 353–361, 2006.
37. Wagner VE and Bryers JD. Poly(ethylene glycol)-polyacrylate copolymers modified to control adherent monocyte-macrophage physiology: interactions with attaching *Staphylococcus epidermidis* or *Pseudomonas aeruginosa* bacteria. *J Biomed Mater Res* 69: 79–90, 2004.
38. Winslow RM. Current status of oxygen carriers (“blood substitutes”): 2006. *Vox Sang* 91: 102–110, 2006.
39. Yoshioka N and Atassi MZ. Haemoglobin binding with haptoglobin: localization of the haptoglobin-binding sites on the beta-chain of human haemoglobin by synthetic overlapping peptides encompassing the entire chain. *Biochem J* 234: 453–456, 1986.

Address reprint requests to:  
 Dominik J. Schaer  
 Medical Clinic Research Unit,  
 University Hospital  
 CH-8091 Zurich, Switzerland  
 E-mail: dominik.schaer@usz.ch

Date of first submission to ARS Central, January 17, 2008, date of final revised submission, February 14, 2008; date of acceptance, February 27, 2008.

**This article has been cited by:**

1. Magnus G. Olsson , Maria Allhorn , Leif Bülow , Stefan R. Hansson , David Ley , Martin L. Olsson , Artur Schmidtchen , Bo Åkerström . 2012. Pathological Conditions Involving Extracellular Hemoglobin: Molecular Mechanisms, Clinical Significance, and Novel Therapeutic Opportunities for #1-Microglobulin. *Antioxidants & Redox Signaling* **17**:5, 813-846. [[Abstract](#)] [[Full Text HTML](#)] [[Full Text PDF](#)] [[Full Text PDF with Links](#)]
2. J. H. Baek, Y. Zhou, D. R. Harris, D. J. Schaer, A. F. Palmer, P. W. Buehler. 2012. Down Selection of Polymerized Bovine Hemoglobins for Use as Oxygen Releasing Therapeutics in a Guinea Pig Model. *Toxicological Sciences* **127**:2, 567-581. [[CrossRef](#)]
3. Paul W. Buehler , Elena Karnaukhova , Monique P. Gelderman , Abdu I. Alayash . 2011. Blood Aging, Safety, and Transfusion: Capturing the “Radical” Menace. *Antioxidants & Redox Signaling* **14**:9, 1713-1728. [[Abstract](#)] [[Full Text HTML](#)] [[Full Text PDF](#)] [[Full Text PDF with Links](#)]
4. Abdu I. Alayash. 2011. Haptoglobin: Old protein with new functions. *Clinica Chimica Acta* **412**:7-8, 493-498. [[CrossRef](#)]
5. Oana Zolog, Augustin Mot, Florina Deac, Alina Roman, Eva Fischer-Fodor, Radu Silaghi-Dumitrescu. 2011. A New Polyethyleneglycol-Derivatized Hemoglobin Derivative with Decreased Oxygen Affinity and Limited Toxicity. *The Protein Journal* **30**:1, 27-31. [[CrossRef](#)]
6. F. Deac, B. Iacob, E. Fischer-Fodor, G. Damian, R. Silaghi-Dumitrescu. 2011. Derivatization of haemoglobin with periodate-generated reticulation agents: evaluation of oxidative reactivity for potential blood substitutes. *Journal of Biochemistry* **149**:1, 75-82. [[CrossRef](#)]
7. F. Vallelia, C. A. Schaer, T. Kaempfer, P. Gehrig, E. Duerst, G. Schoedon, D. J. Schaer. 2010. Glucocorticoid treatment skews human monocyte differentiation into a hemoglobin-clearance phenotype with enhanced heme-iron recycling and antioxidant capacity. *Blood* **116**:24, 5347-5356. [[CrossRef](#)]
8. Ryan B. Huang, Supriya Mocherla, Michael J. Heslinga, Phapanin Charoenphol, Omolola Eniola-Adefeso. 2010. Dynamic and cellular interactions of nanoparticles in vascular-targeted drug delivery (review). *Molecular Membrane Biology* **27**:7, 312-327. [[CrossRef](#)]
9. Paul W. Buehler, Felice D’Agnillo, Dominik J. Schaer. 2010. Hemoglobin-based oxygen carriers: from mechanisms of toxicity and clearance to rational drug design. *Trends in Molecular Medicine* **16**:10, 447-457. [[CrossRef](#)]
10. Ryan B. Huang, Supriya Mocherla, Michael J. Heslinga, Phapanin Charoenphol, Omolola Eniola-Adefeso. 2010. Dynamic and cellular interactions of nanoparticles in vascular-targeted drug delivery (review). *Molecular Membrane Biology* **27**:4-6, 190-205. [[CrossRef](#)]
11. Abdu I. Alayash. 2010. Setbacks in Blood Substitutes Research and Development: A Biochemical Perspective. *Clinics in Laboratory Medicine* **30**:2, 381-389. [[CrossRef](#)]
12. John D. Belcher , Joan D. Beckman , Gyorgy Balla , Jozsef Balla , Gregory Vercellotti . 2010. Heme Degradation and Vascular Injury. *Antioxidants & Redox Signaling* **12**:2, 233-248. [[Abstract](#)] [[Full Text HTML](#)] [[Full Text PDF](#)] [[Full Text PDF with Links](#)]
13. Andrew P. Levy , Rabea Asleh , Shany Blum , Nina S. Levy , Rachel Miller-Lotan , Shiri Kalet-Litman , Yefim Anbinder , Orit Lache , Farid M. Nakhoul , Roy Asaf , Dan Farbstein , Mordechai Pollak , Yitzhak Z. Soloveichik , Merav Strauss , Jonia Alshiek , Alina Livshits , Avery Schwartz , Hoda Awad , Kheir Jad , Hagit Goldenstein . 2010. Haptoglobin: Basic and Clinical Aspects. *Antioxidants & Redox Signaling* **12**:2, 293-304. [[Abstract](#)] [[Full Text HTML](#)] [[Full Text PDF](#)] [[Full Text PDF with Links](#)]
14. Rebecca L. Rich, David G. Myszk. 2010. Grading the commercial optical biosensor literature-Class of 2008: ‘The Mighty Binders’. *Journal of Molecular Recognition* **23**:1, 1-64. [[CrossRef](#)]
15. Felicitas S. Boretti, Paul W. Buehler, Felice D’Agnillo, Katharina Kluge, Tony Glaus, Omer I. Butt, Yiping Jia, Jeroen Goede, Claudia P. Pereira, Marco Maggiorini, Gabriele Schoedon, Abdu I. Alayash, Dominik J. Schaer. 2009. Sequestration of extracellular hemoglobin within a haptoglobin complex decreases its hypertensive and oxidative effects in dogs and guinea pigs. *Journal of Clinical Investigation* . [[CrossRef](#)]
16. Tatiana Pimenova, Claudia P. Pereira, Dominik J. Schaer, Renato Zenobi. 2009. Characterization of high molecular weight multimeric states of human haptoglobin and hemoglobin-based oxygen carriers by high-mass MALDI MS. *Journal of Separation Science* **32**:8, 1224-1230. [[CrossRef](#)]
17. P. W. Buehler, B. Abraham, F. Vallelia, C. Linnemayr, C. P. Pereira, J. F. Cipollo, Y. Jia, M. Mikolajczyk, F. S. Boretti, G. Schoedon, A. I. Alayash, D. J. Schaer. 2009. Haptoglobin preserves the CD163 hemoglobin scavenger pathway by shielding hemoglobin from peroxidative modification. *Blood* **113**:11, 2578-2586. [[CrossRef](#)]

18. Florence Vallelian, Tatiana Pimenova, Claudia P. Pereira, Bindu Abraham, Malgorzata G. Mikolajczyk, Gabriele Schoedon, Renato Zenobi, Abdu I. Alayash, Paul W. Buehler, Dominik J. Schaer. 2008. The reaction of hydrogen peroxide with hemoglobin induces extensive  $\alpha$ -globin crosslinking and impairs the interaction of hemoglobin with endogenous scavenger pathways. *Free Radical Biology and Medicine* **45**:8, 1150-1158. [[CrossRef](#)]